Acta Polytechnica CTU Proceedings **55**:56–62, 2025
https://doi.org/10.14311/APP.2025.55.0056

Published by the Czech Technical University in Prague

NUMERICAL SIMULATION OF SECONDARY HEAT EXCHANGER IN S-ALLEGRO

Adam Palouda[a, b]

[a] *Technical University of Liberec, Faculty of Mechanical Engineering, Department of Power Engineering, Studentská 1402/2, 461 17 Liberec, Czech Republic*

[b] *UJV Řež a.s, Hlavní 130, 250 68 Husinec – Řež, Czech Republic*

correspondence: adam.palouda@ujv.cz

Abstract. This paper presents a computational analysis of the Secondary Heat Exchanger (SHX) in the S-Allegro experimental facility. The S-Allegro facility is a helium circuit which serves as an experimental platform for validating thermohydraulic calculations of helium flow in support of Gas-cooled Fast Reactor (GFR) development. A computational analysis performed on the SHX included calculations using criterial equations of heat transfer and, most importantly, numerical simulation. Both methods were compared to experimental data and adjusted to achieve a good agreement. The results of the numerical simulations are used to analyse flows in the heat exchanger and identify potential improvements in future design of heat exchangers for GFR. The study provides insights into the thermal performance of helium-water heat exchangers and contributes to the validation of computational methods for GFR technology development.

Keywords: CFD, GFR, Gas-cooled Fast Reactor, heat exchanger, nuclear power, numerical simulations.

1. Introduction

This paper focuses on heat exchangers in Gas-cooled Fast Reactors (GFRs), which are considered one of the most promising technologies for the future of nuclear energy because of following advantages [1]: GFRs have the potential to address several of the most pressing problems in nuclear energy, including nuclear fuel issues and the risk of nuclear accidents. Nuclear fuel presents challenges both in terms of fresh uranium mining and spent fuel storage, both of which GFR technology has the potential to resolve. GFRs can operate as breeder reactors, meaning they can produce more fissile material than they consume. In simplified terms, GFRs can recycle spent nuclear fuel while still generating energy from it. Additionally, these reactors should incorporate many more passive safety features, thus virtually eliminating the possibility of nuclear accidents. Other advantages include the ability to use GFR not only for highly efficient electrical energy production but also for hydrogen production or as a heat source for industrial applications.

The development of GFR technology involves numerous challenges, primarily related to high coolant temperatures and high neutron flux. One of these challenges is the construction of heat exchangers, which is more demanding compared to water-cooled nuclear power plants. This is due to helium's inferior heat transfer properties compared to water, as well as higher operating temperatures that place increased demands on materials and technologies used.

To investigate problematic areas in GFR development and verify new concepts, the Allegro demonstration reactor project was created. This reactor will not generate electricity but will serve for research and support the licensing of future power plants with GFR reactors. One of these planned reactors is being developed in the Czech Republic by ÚJV Řež under the name HeFASTo. Development of Allegro is currently underway with intensive efforts. As part of its development and licensing preparation V4G4 Center of Excellence consortium built the S-Allegro facility in the Czech Republic under the auspices of the Sustainable Energetics (SUSEN) project [2].

This facility is an electrically heated scaled-down version of Allegro at a 1:75 power scale, which maintains similar thermohydraulic properties using similarity theory. This facility enables experimental validation and verification of thermohydraulic operation and safety of GFR-type reactors. Figure 1 shows a layout of the S-Allegro facility. On the layout you can see the reactor pressure vessel, which is actually an electrical heater simulating a reactor, and heat exchangers (HX) and circulators of primary, secondary and DHR (Decay Heat Removal) loops.

This paper describes a computational analysis of flow and heat transfer in the Secondary Heat Exchanger (SHX) which connects secondary and tertiary circuits of the S-Allegro. The performed analysis is subsequently compared with experimental data from S-Allegro facility operation, enabling verification of its correctness. The purpose of this analysis is to thoroughly investigate heat exchanger operation and verify the functionality of the computational methods used, potentially modifying the methods to achieve the best possible agreement between calculations and

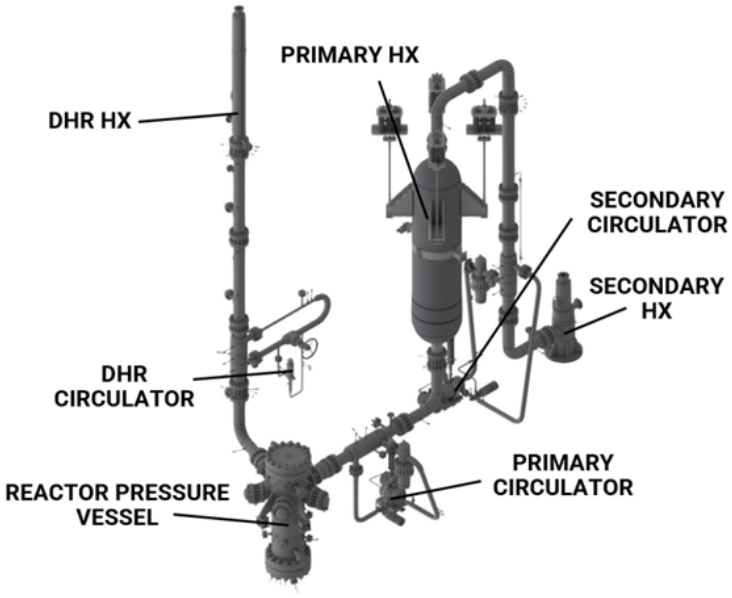

FIGURE 1. Layout of S-Allegro [3].

reality. Analysed heat exchanger is a Tube-and-Shell type and it uses hot helium and cold water as working fluids. Figure 2 shows the flow routes in the SHX.

2. METHODOLOGY

2.1. EXPERIMENTAL SETUP AND OPERATING CONDITIONS

Two steady-state operating conditions (called Steady State 1 and Steady State 2) of the heat exchanger were selected for validation purposes, with experimental data obtained from a measurement campaign which was part of Safe-G research project [4].

The experimental parameters for both operating conditions are summarized in Table 1. Steady State 1 operates with lower helium mass flow ($0.20\,\mathrm{kg\,s^{-1}}$) and higher inlet temperature (390.8 K), while Steady State 2 employs higher helium mass flow ($0.50\,\mathrm{kg\,s^{-1}}$) with lower inlet temperature (355.5 K). Both conditions maintain similar water flow rates ($\sim 2.8\,\mathrm{kg\,s^{-1}}$) and inlet temperatures ($\sim$295 K).

The table only shows inlet parameters of both fluids, because these are required to perform the calculations. Outlet parameters of both fluids are later used to determine whether the calculations agree with the experiment. For both methods (criterial equation calculations and numerical simulation), the study first deals with the Steady State 1. The results of the calculations are being compared to the experiments and the methods are adjusted to achieve a better agreement. After achieving good agreement with experimental data for Steady State 1 by adjusting both methods, the same calibrated methods were applied without further modification to Steady State 2. The comparison with experimental results in this second operating state serves to evaluate how well the adjusted models can predict the heat exchanger's behavior under different conditions.

2.2. CRITERIAL CALCULATIONS

First, a calculation of the heat exchanger using criterial equations was performed. The calculation was performed using the logarithmic mean temperature difference with corrections (e.g., for the effect of multipass). A script was written in MATLAB for the calculation. The physical properties of helium are input into the script using NIST [5] data for average temperature and pressure in the heat exchanger. Using average values introduces some error but given the small changes in helium physical properties in the given temperature range, it is acceptable. For the same reason, it is also possible to neglect the fact that some criterial equations were derived for the average of free stream temperature and wall temperature, while here the free stream temperature is used. For water, physical properties are input from the XSteam [6] database, also for average temperature and pressure.

For calculating the Nusselt number on the helium side, a relationship for forced convection inside a tube was used. Since this is one of the most common distributions for which heat transfer is calculated, a large number of different criterial equations are available in the literature. Since these criterial equations were derived from straight tube experiments, using them for the U-tubes in the heat exchanger may introduce some error. Thanks to having an experiment available for comparison, several different criterial equations were tested. The equation that gave results most accurately matching the experiment (Steady State 1) was selected:

$$Nu = 0.023 \cdot Re^{0.8} \cdot Pr^{0.4}, \tag{1}$$

Route	Description
1	Secondary helium side (hot side) inlet. D = 91.6 mm.
2	Tube side, secondary helium, the main heat exchanging part. 57 × U-tube, OD 16 mm, ID 11 mm, average tube length 1.588 m, average tubes pitch 21 mm.
3	Secondary helium side (hot side) outlet. Annulus ID = 168.3 mm, OD 193.7.
1	Tertiary water side (cold side) inlet. ID 107.1 mm, length 0.2 m.
2	Tertiary water side – shell side, the main heat exchanging part. ID 285 mm. 6 baffles to ensure cross flow. Baffles vertical pitch 100 mm.
3	Tertiary water side (cold side) inlet. ID 107.1 mm, length 0.15 m.

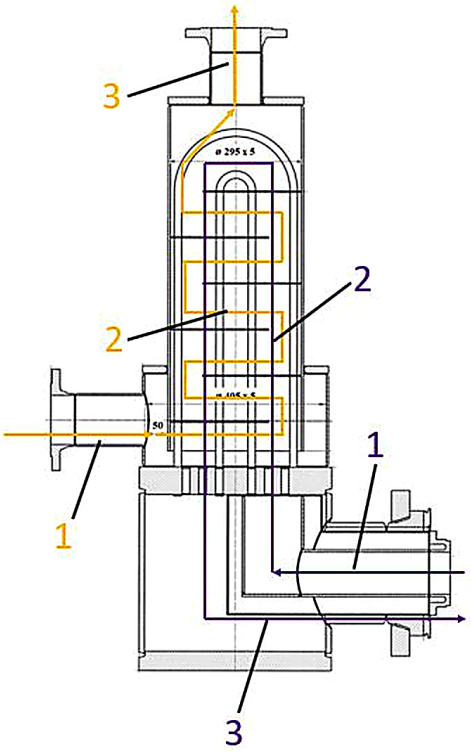

Figure 2. Flow routes in Secondary Heat Exchanger [3].

Parameter	**Steady State 1**	**Steady State 2**
Helium pressure [MPa]	3.5 ± 0.1	3.5 ± 0.1
Helium mass flow [kg s^{-1}]	0.20 ± 0.01	0.50± 0.02
Helium inlet temperature [K]	390.8 ± 0.5	355.5 ± 0.3
Water pressure [MPa]	0.58 ± 0.01	0.57 ± 0.01
Water mass flow [kg s^{-1}]	2.79 ± 0.03	2.76 ± 0.03
Water inlet temperature [K]	293.5 ± 0.1	295.9 ± 0.1

Table 1. Experimental data from SHX operation.

where Nu is Nusselt number, Re is Reynold number and Pr is Prandtl number [7]. This equation, known as the Dittus–Boelter equation, is valid for flows with a Prandtl number ranging from 0.6 to 160 and a Reynolds number greater than 10 000. Both experiments meet these criteria, with a Prandtl number of approximately 0.65 and Reynolds numbers of approximately 16 000 (Steady State 1) and 45 000 (Steady State 2).

For water, the values of characteristic numbers number and heat transfer coefficient was calculated as average for the entire heat exchanger using the procedure specific to the given heat exchanger type and geometry according to the VDI Heat Atlas [7].

2.3. Numerical simulation

First step of the numerical simulation preprocessing was creating a 3D geometry of the heat exchanger. This was done from the technical drawings provided by the manufacturer. Autodesk Inventor computer program was used for creating the geometry. Several minor alterations were made to the geometry to make the simulations work more smoothly. For example the outlet pipeline was prolonged to allow simulating an eddy at the outlet which was revealed in first preliminary simulations. The geometry was made in half symmetry to save computational demand of the simulation.

The numerical simulation was carried out using ANSYS Fluent. The numerical simulation was solved as conjugate heat transfer, combining both conduction and convection. Three different approaches to this problem formulation were tested:

The first approach involves creating a conformal computational mesh where the computational grids of individual media (helium, solid wall, water) meet at nodal points. Such a mesh automatically assumes heat transfer from one medium to another.

The second approach utilizes a non-conformal computational mesh where the grids of individual media

have different nodal points at the contact interface. In this case, heat transfer must be prescribed through boundary conditions.

The third option is referred to as the "thin-wall" approach, where the solid wall has no computational mesh or volume of its own, and the space it occupies in reality is filled with one of the flowing media in the simulation. The thermal resistance of heat conduction is then incorporated into the simulation through boundary conditions.

A coarse computational mesh was generated for each method and simulations were performed. Based on these preliminary simulations, the conformal mesh was selected as the most suitable approach for this study. Its primary advantages include straightforward simulation setup and the fact that it does not distort the solved problem. The "thin-wall" method enables significant reduction in mesh cell count and consequently computational demand, but at the expense of altering the actual flow geometry, resulting in slight solution distortion (estimated at approximately 2.5 % error based on correlational calculations in this case). The non-conformal mesh could also reduce cell count but its disadvantage lies in the very laborious setup procedure.

Due to the relatively complex geometry of the heat exchanger, a large number of cells was required for computational mesh generation. The first mesh created, which was sufficiently fine to enable proper flow simulation within the heat exchanger, consisted of 250 million cells. Such a large computational mesh could not be simulated using the available computational resources. Therefore, approaches were sought to reduce the cell count while maintaining adequate mesh refinement.

One approach involved modifying the heat conduction calculation through tube walls. While accurate modeling typically requires several cell layers to capture the logarithmic temperature profile in cylindrical walls, this would significantly increase cell count. Therefore, a modification was implemented where the wall is modeled using only a single cell layer with thermal conductivity increased to $200\,\mathrm{W\,(m\,K)^{-1}}$ (approximately 10 times higher than stainless steel from which the tubes are actually made), virtually eliminating wall thermal resistance. This resistance is then incorporated through boundary condition calculations on both tube surfaces. Unlike the "thin-wall" approach, this method maintains actual geometry without distortion. Validation using a simplified tube model showed acceptable accuracy with only 0.17 % difference in heat transfer rate compared to conventional modeling. This approach allowed very significant reduction of mesh cells.

With this and some other alterations a mesh consisting of 29 million cells was created. Average value of Element Quality was 0.77 with the worst value being 0.03. This low quality of some cells could cause calculation errors but the results were thoroughly examined to make sure no singularities or other problems appeared. Figure 3 shows the created mesh for the simulation.

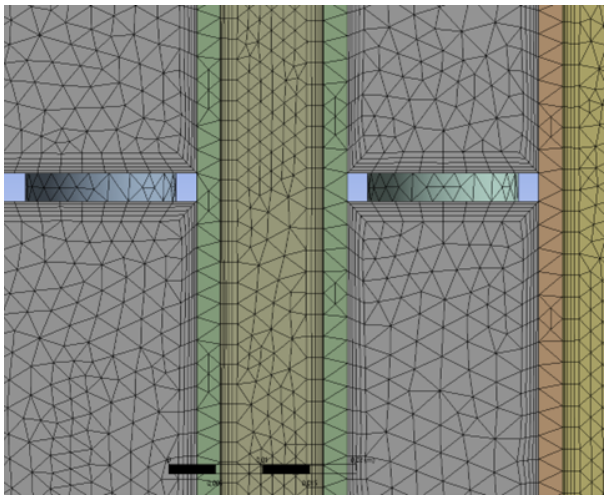

FIGURE 3. Representative section of the computational mesh of the simulation.

Two turbulence models were employed for comparison: k-ω SST and k-ε realizable, both known for their good performance in heat transfer applications. Achieved data were compared with experimental data from Steady State 2 and k-ω SST showed a better agreement. Therefore only this model was used for Steady State 2.

Boundary conditions were carefully specified to match experimental conditions. For both steady states, helium inlet conditions included mass flow rate, temperature, and turbulence parameters (5 % intensity, 11 mm hydraulic diameter). Water inlet conditions similarly specified mass flow rate, temperature, and turbulence parameters (5 % intensity, 107 mm hydraulic diameter). Both outlets were specified as pressure outlets with zero backpressure and 300 K backflow temperature.

Wall boundary conditions included no-slip smooth walls for all fluid-solid interfaces. Heat conduction through the tube walls was modeled using coupled boundary conditions with a wall thickness of 1.25 mm on both inner and outer diameter. Material properties were specified using NIST data for helium and Fluent database for water, with steel thermal conductivity of $20\,\mathrm{W\,(m\,K)^{-1}}$ used in the boundary condition calculation.

The SIMPLEC algorithm was employed for pressure-velocity coupling, with second-order upwind discretization schemes for all variables except pressure, which used the PRESTO! scheme. Under-relaxation factors were set to 0.3 for pressure, 0.7 for momentum, and 1.0 for energy to ensure numerical stability.

Parameter	Experiment	Criterial	k-ω SST	k-ε Realizable
Helium outlet temperature [K]	313.5	313.3	311.0	310.0
Water outlet temperature [K]	300.1	300.1	300.3	300.3
Heat transfer coefficient - water [W (m^2 K)$^{-1}$]	-	3 180	3 253	3 707
Heat transfer coefficient - helium [W (m^2 K)$^{-1}$]	-	788	950	969
Thermal output [kW]	79.8	79.4	81.5	82.4

Table 2. Steady State 1 comparison results.

3. Results and discussion

3.1. Steady State 1 results

The numerical simulation results for Steady State 1 demonstrated good agreement with experimental data, as shown in Table 2. Both turbulence models predicted helium outlet temperatures within 3.5 K of the experimental value (313.5 K), with the k-ω SST model showing slightly better agreement (311.0 K vs. 310.0 K for k-ε). Water outlet temperatures were predicted with excellent accuracy, within 0.3 K of the experimental value (300.1 K). Criterial calculations achieved extremely good agreement where within the difference of 0.2 K at helium outlet temperature. This was achieved because several criterial equations for calculation heat transfer coefficient were tested and the one with best results was used. Others varied within 5 %. We can see differences in heat transfer coefficients calculated by different methods. These are not unusual since forced convection can only be predicted with limited precision. The reason why the difference in outlet temperatures is relatively smaller compared to the difference in heat transfer coefficients is that the temperatures of helium and water are almost matched at the outlet so intensity of heat transfer becomes less intensive Figure 4 shows the temperature contour in the symmetry plane of the heat exchanger. Figure 5 presents the water flow vector map, which was used to analyze design of the exchanger and propose some improvements (described later in the text).

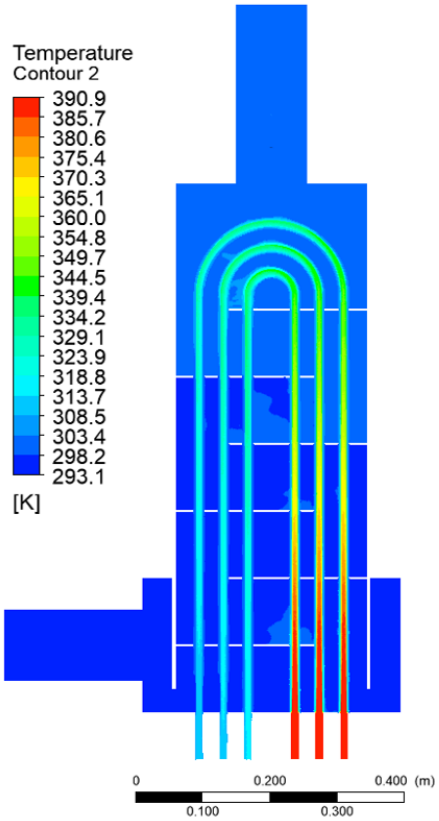

Figure 4. Temperature contour in the symmetry plane of the heat exchanger.

3.2. Steady State 2 results

Steady State 2 results, summarized in Table 3, demonstrated similarly good (even slightly better) agreement between both calculation methods and experimental data. The very good agreement of both heat transfer coefficients between CFD simulation and criterial calculation enhances the credibility of the results. The reason why the agreement is better than in Steady State 1 might be related to y+ parameter. This parameter describes how finely the mesh can capture turbulent effects in the fluid flow near wall. In Steady State 1, the average value of y+ is 7.7 at helium side while in Steady State 2 it is 16.3 (because of higher helium velocities). On the water side y+ values were very similar in both steady states and also the heat transfer coefficients matched similarly good. The available literature recommends not to use meshes with y+ values between 5 and 15 [8] and to test this a mesh sensitivity study on one helium tube was done reaching similar conclusion.

3.3. Design improvement proposals

Numerical simulation provides valuable insights beyond overall heat transfer data, including velocity field maps useful for design analysis. Analysis of water flow near the heat exchanger outlet revealed a low-velocity region close to the outlet where heat transfer intensity decreases despite high helium temperature and significant heat transfer surface area at the tube bend. Additionally, an eddy in the outlet piping increases pressure losses. Both issues could be addressed by adding baffles, modifying existing baffle positions, or chamfering the cylindrical body edge. Numerical simulations were conducted for two possible modifications: edge chamfering and baffle addition (shown in Figure 6). The added baffle must be shorter than others

Parameter	Experiment	Criterial	CFD
Helium outlet temperature [K]	318.4	317.0	317.5
Water outlet temperature [K]	304.5	304.5	304.3
Heat transfer coefficient - water [W (m^2 K)$^{-1}$]	-	3 173	3 191
Heat transfer coefficient - helium [W (m^2 K)$^{-1}$]	-	1 653	1 687
Thermal output [kW]	99.2	99.3	97.7

TABLE 3. Steady State 2 comparison results.

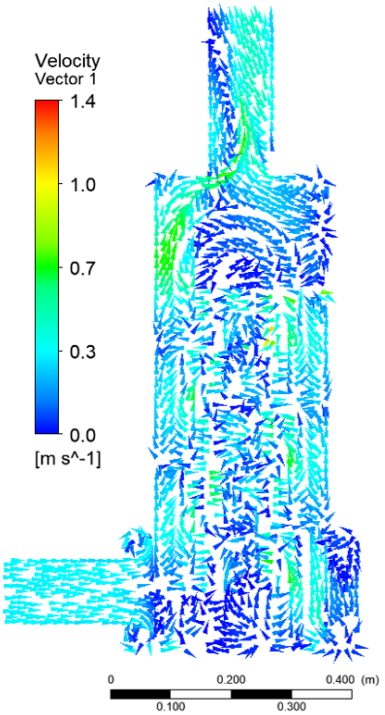

FIGURE 5. Water flow velocity vector field in the symmetry plane of the heat exchanger.

due to assembly complications at the tube bend location. The shortened baffle improved flow at tube bends and eliminated outlet vortex. However, comprehensive simulations including heat transfer are needed before definitive conclusions can be drawn. These possible changes are not mentioned to be implemented in the current heat exchanger but rather in future design in upgrading S-Allegro, or developing Allegro reactor.

4. CONCLUSIONS

This study presented a computational analysis of the secondary heat exchanger in the S-Allegro experimental facility, comparing results obtained using empirical correlation-based calculations (criterial equations) and CFD numerical simulations against experimental data. The results suggest that both computational approaches can provide reasonable predictions of heat exchanger performance. Both methods showed a good agreement with experimental data of two different steady states – the first one was used to develop the method and the second one to test it. The somewhat better agreement of CFD observed for Steady

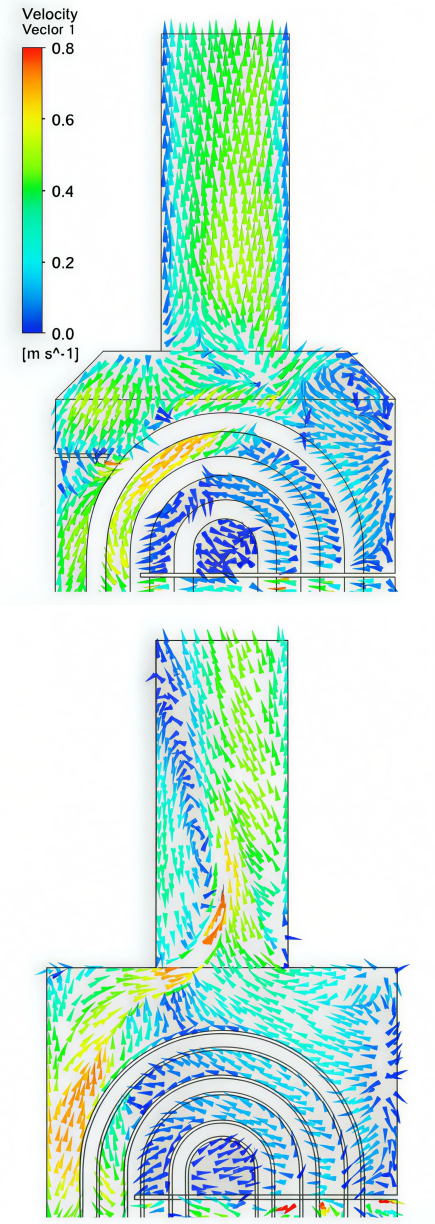

FIGURE 6. Comparison of water velocity vector fields close to the outlet. Top: Proposed improvement, Bottom: Original.

State 2 may be related to mesh quality parameters, specifically the y+ values, which appeared more favorable for the higher flow rate conditions. While both methods showed high correlation with experimental

data, it is important to acknowledge the inherent limitations of computational approaches. Many factors can influence results. The observed variations in heat transfer coefficients between different calculation methods highlight the uncertainties associated with predicting heat transfer. The CFD analysis provided valuable insights into flow patterns within the heat exchanger, revealing an area of low-velocity flow near the outlet that could potentially be improved through design modifications such as baffle repositioning or edge chamfering. However, these proposed improvements would require comprehensive validation through additional simulations and experimental testing before implementation. Their implementation to the current heat exchanger is not likely, but the suggestions might be used in design of other heat exchangers in GFR development. This work contributes to the validation of computational methods for analyzing helium-water heat exchangers in support of Gas-cooled Fast Reactor development. The reasonably good agreement between calculations and experiments suggests that these methods can serve as useful tools for heat exchanger design and optimization, while recognizing that experimental validation remains essential for confirming computational predictions.

Acknowledgements

The author would like to thank his thesis supervisor Jan Kracík for his guidance and support throughout this research. Special appreciation is extended to colleagues at ÚJV Řež for their support and collaboration, especially Jan Komrska, Petr Vácha and Ondřej Krejčí. The author also gratefully acknowledges the S-Allegro facility team for providing experimental data that made this validation study possible.

References

[1] Generation IV International Forum. Gas-cooled Fast Reactor (GFR). [2025-09-19]. https://www.gen-4.org/generation-iv-criteria-and-technologies/gas-cooled-fast-reactor-gfr

[2] ALLEGRO. ALLEGRO Project – Gas-cooled Fast Reactor Demonstrator. [2025-09-19]. https://allegroreactor.cz/

[3] T. Melichar, J. Šefl, D. Kříž. *SafeG – DELIVERABLE D5.3 (Definition of the Thermal-Hydraulic Benchmark.* CVŘ, Husinec – Řež, 2023.

[4] B. Kvizda. *Results of the thermal-hydraulics benchmark. SafeG – Deliverable D5.4.* VUJE a.s., Trnava, 2020.

[5] National Institute of Standards and Technology. NIST WebBook Chemistry SRD 69, 2023. [2025-04-08]. https://webbook.nist.gov/cgi/fluid.cgi?TUnit=C&PUnit=MPa&DUnit=kg/m3&HUnit=kJ/kg&WUnit=m/s&VisUnit=Pa*s&STUnit=N/m&Type=IsoBar&RefState=DEF&Action=Page&ID=C7440597

[6] M. Holmgren. X Steam, Thermodynamic properties of water and steam. MATLAB central file exchange, 2025. [2025-02-12]. https://www.mathworks.com/matlabcentral/fileexchange/9817-x-steam-thermodynamic-properties-of-water-and-steam

[7] VDI Gesellschaft. *VDI Heat Atlas.* Springer, Berlin, 2010. ISBN 978-3-540-77876-9.

[8] ANSYS, Inc. Ansys Fluent user's guide. Release 2023 R1. ANSYS, Inc., Canonsburg, PA, 2023.